Original Article

Theoretical deposition of random walk-generated nanoaggregates in the lungs of healthy males and females

Robert Sturm

Department of Chemistry and Physics of Materials, University of Salzburg, Salzburg, Austria

Correspondence to: Dr. Robert Sturm. Brunnleitenweg 41, 5061 Elsbethen, Austria. Email: sturm_rob@hotmail.com.

Background: Particle aggregates with different complexity and size represent an essential component of the ambient atmosphere. Therefore, theoretical knowledge on the effects of this particle group in the human respiratory tract is indispensable. In the present study an innovative model for the hypothetical generation of such aggregates is described in detail. In addition, lung deposition of the computed particles was predicted for both male and female subjects.

Methods: The theoretical approach used in this contribution is based on a random-walk algorithm allowing the construction of aggregates with cluster-, chain- or disk-like geometry. Basic components of these complex particulate structures are represented by monodisperse spheres with a diameter of 1 nm. These spherical elements were sticked together by random walks consisting of 10, 100 or 1,000 steps, resulting in aggregates of different size and complexity. Deposition calculations were carried out by assuming (I) a stochastic structure of the human respiratory tract and (II) different physical mechanisms seizing the inhaled particles.

Results: Under sitting breathing conditions total deposition of variably sized nanoaggregates ranges from 98.9% to 100% in males and from 98.6% to 100% in females. In the extrathoracic region particle accumulation amounts to 39.3–64.6% (males) and 40.4–64.1% (females), whereas bronchial deposition adopts values of 20.4–44.6% (males) and 20.9–43.2% (females). Alveolar deposition can be estimated at 1.68–14.9% in males and 1.58–18.4% in females. Gender-specific differences of generation-by-generation deposition of nanoaggregates are on the order of 0–0.5%.

Conclusions: According to the results of the study deposition of nanoaggregates in the human respiratory tract strongly depends on the size of the inhaled particulate structures. In addition, partly significant differences of pulmonary particle accumulation between male and female subjects can be determined. All these circumstances have to be considered with regard to the formulation of respective health risk assessments.

Keywords: Nanoaggregates; random-walk model; inhalation; lung deposition; males; females

Received: 27 March 2018; Accepted: 23 April 2018; Published: 26 April 2018.

doi: 10.21037/jphe.2018.04.02

View this article at: http://dx.doi.org/10.21037/jphe.2018.04.02

Introduction

The ambient atmosphere is characterized by the content of numerous particulate substances varying in both size and shape. Among this multitude of airborne particles aggregates of the nanometer- and micrometer-scale exhibit a highly specific aerodynamic behavior (1-5). Previous research studies (3-7) yielded evidence that transport of aggregates in various regions of the human respiratory tract deviates remarkably from that of ideal spheres with comparable volume-equivalent diameter. A considerable fraction of particle aggregates either originates from incomplete combustion or may be regarded as result of extremely fast agglomeration processes such as explosive chemical reactions. These particulate structures, however,

are commonly marked by dynamic shape factors adopting values between 2 and 15 (2,4), so that their aerodynamic properties are largely comparable to those of carbon nanotubes with extreme aspect ratios (8-12) or ultrathin graphene nanoplatelets (13,14).

Due to their small sizes and exceptional aerodynamic characteristics nano-scale aggregates preferably accumulate in the large airway structures of the upper respiratory tract, where they are driven towards the airway walls by Brownian motion. Micro-scale aggregates, on the other hand, show a rather indifferent deposition behavior which is distinguished by almost identical accumulation rates in the central and peripheral lung compartments (4,5,13-16).

For highly appropriate model predictions of aggregate deposition in the bronchial and alveolar structures of the human lungs generation of particulate bodies with realistic sizes and shapes represents a basic requirement. In previous studies generation of complex aggregates was among other carried out with the help of stochastic approaches (4-7). These models, however, crystallized out as advantageous with regard to the definition of many different particle geometries, but, on the other hand, required rather large-scale mathematical computations. According to comprehensive microscopic investigations aggregate structures belonging to different size categories usually contain high amounts of small isometric components. These elements are assembled to anisometric objects with cluster-, chain- or platelet-like geometries (2,3,17,18). In numerous cases single components of an aggregate originating from chemical processes are distinguished by equal diameters, whereas aggregates formed by electrostatic processes may be marked by high geometric inhomogeneity of their components (1-5).

The present contribution pursues two main objectives: first, an innovative method of aggregate generation based on the random-walk concept (19) is described in detail. This approach allows the theoretical construction of aggregates with different sizes, shapes and complexities, whereby highly intricate mathematical calculations can be omitted. Second, deposition behavior of the random-walk aggregates is investigated for both male and female lungs. According to previous studies (20,21) the human respiratory tract is characterized by a gender-specific morphometry (i.e., female lungs are slightly smaller than male ones). Additional discrepancies in breathing behavior commonly result in very individual deposition rates of the inhaled particles.

Methods

Aggregate generation according to the random-walk concept

As already outlined by Sturm (19), computer-aided generation of particle aggregates is based on a simple algorithm. Computation starts with placing the first component of the aggregate at the origin of a three-dimensional Cartesian coordinate system. Subsequently, steps with absolute lengths of –1, 0 or +1 units are calculated along the three spatial directions. Thereby, adoption of a specific value is determined by the random-number concept. The currently generated position is occupied by a new component. If the computed coordinate is already claimed by another component, the software checks the number of steps computed so far. If this number remains under a maximal step number (e.g., 1,000) constituted for the specific aggregate, a new position for the component of interest is modeled according to the procedure described above. If, on the other hand, this maximal step number is attained, construction of the aggregate is terminated and essential aerodynamic parameters of the produced particulate structure are calculated. Continuous spatial arrangement of monodisperse spherical components results in the growth of the aggregate and successive enhancement of its structural complexity (*Figure 1*).

The random-walk algorithm outlined above was realized by using the largely distributed software MS EXCEL™. In this computer program, which was originally developed for economic calculations, the user can immediately visualize the results obtained from the theoretical computations. For this study complex aggregates consisting of 10, 100 and 1,000 random-walk steps were generated (*Figure 1*). In this context isometric growth of the particulate structures along the three axes of the coordinate system was assumed, resulting in almost isodimensional clusters. Additionally, it has to be noted that any increase of the growth probabilities along two spatial directions with respect to the growth probability along the third direction leads to the generation of platelet-like aggregate geometries. On the other hand, a significant decline of the growth probabilities along those coordinate axes with respect to the probability along the third direction induces the production of chain-like aggregates (19).

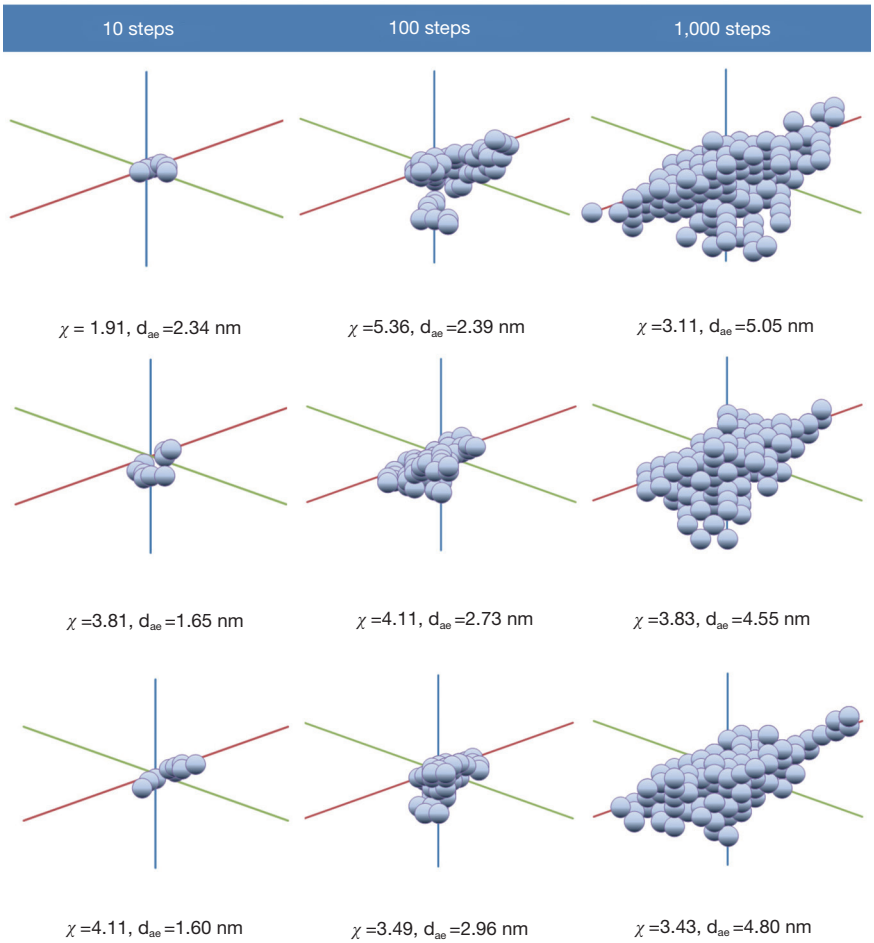

Figure 1 Examples of nanoaggregate generation with the random-walk model (see text for further details). Whilst smallest aggregates considered in this study consist of 10 random-walk steps, largest aggregates include 1,000 random-walk steps. Respective aerodynamic parameters calculated for the single particulate structures have been added.

Deposition of nanoaggregates in male and female lungs

Deposition computations presented in this contribution were limited to nanoaggregates assuming a maximal size of 0.1 µm. For this purpose basic spherical components with a uniform diameter of 1 nm were presupposed. In addition, the aggregates generated according to the random-walk procedure were characterized by unit-density (1 g/cm^3). Simulations of aggregate deposition in the human respiratory tract were carried out by using a stochastic particle transport and deposition program that was subjected to a comprehensive validation and refinement process in the past decades (19-26). Within the stochastic lung architecture single inhaled particles are transported along randomly selected paths and seized by different deposition mechanisms (Brownian motion, inertial impaction, interception, sedimentation). Interaction of these mechanisms commonly determines the particle fractions deposited in the bronchial, bronchiolar and alveolar structures of the respiratory system. Deposition behavior of variably sized aggregates in the airways and alveoli was extrapolated by application of the Monte Carlo method and the mathematical technique of statistical weights (19-28). From the stochastic model information with regard to total, regional and generation-by-generation deposition was extracted (20).

Deposition of nanoaggregates in the respiratory tracts of males and females was carried out by assuming lungs of average size, respectively [FRC (male) =3,300 mL, FRC (female) =2,650 mL; (29)]. Inhalation of particles was

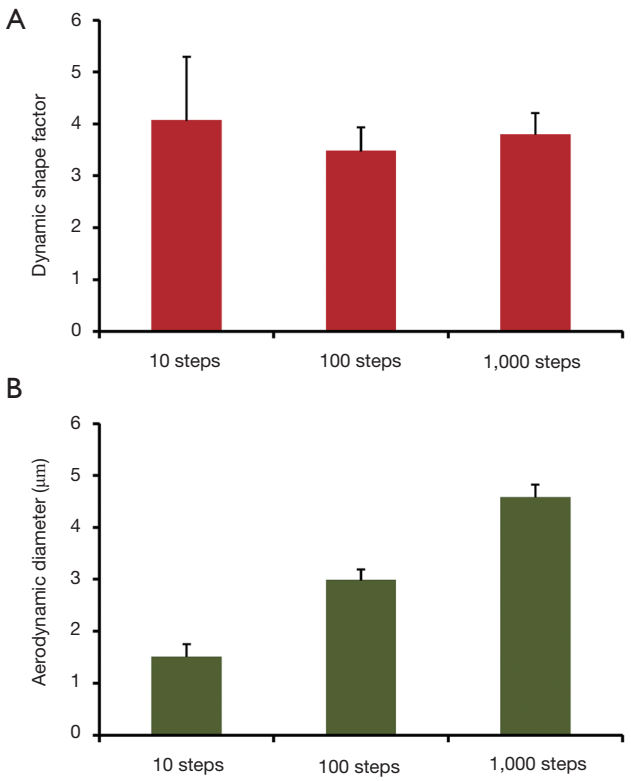

Figure 2 Aerodynamic characteristics (mean ± standard deviation) of nanoaggregates with increasing structural complexity. (A) Dynamic shape factor [calculation according to the mathematical concept outlined by Kasper (2)]; (B) aerodynamic diameter [calculation according to the standard formula introduced by Fuchs (1)].

simulated for sitting breathing conditions with breathing frequencies of 14.4 min^{-1} (male) and 18.5 min^{-1} (female), breath-hold phases of 1 s (male and female) as well as tidal volumes of 750 mL (male) and 625 mL (female).

Results

Aerodynamic properties of random-walk modeled nanoaggregates

Essential parameters describing aggregate aerodynamics in the human respiratory tract are illustrated in *Figure 2*. With regard to the dynamic shape factor, whose computation was carried out according to the concept stated by Kasper (2), aggregates generated by 10 random-walk steps adopt a value of 4.07±1.23. Aggregates consisting of 100 random-walk steps are characterized by a value of 3.48±0.46, whereas largest particulate structures including 1,000 random-walk steps are distinguished by a value of 3.80±0.41 (*Figure 2A*).

Whilst the dynamic shape factor exhibits a rather indifferent behavior with increasing aggregate size and complexity, the aerodynamic diameter positively correlates with the number of random-walk steps used in the model simulations. This phenomenon may be regarded as result of the continuously increasing volume-equivalent diameter (19-29). Smallest aggregates (10 random-walk steps) adopt an aerodynamic diameter of 1.51±0.24 nm, whereas aggregates including 100 random-walk steps have an aerodynamic diameter of 2.99±0.11 nm and thus are twice as large as their smaller counterparts. Aggregates consisting of 1,000 random-walk steps have an aerodynamic diameter of 4.58±0.25 nm, which corresponds to a size increase of 203% compared to the smallest particulate structures (*Figure 2B*).

Deposition of nanoaggregates in male and female lungs

Concerning total and regional (i.e., extrathoracic, bronchial and alveolar) deposition of random-walk-generated aggregates, respective model predictions are summarized in *Figure 3*. In general, total deposition declines from 100% (10 random-walk steps) to 98.9% (1,000 random-walk steps) in the male respiratory tract and from 100% to 98.6% in the female one. Deposition of complex particulate structures in the extrathoracic (nasal) airways commonly exhibits a negative correlation with particle size. In males small aggregates (10 steps) are deposited by 64.6% and large ones (1,000 steps) by 39.3%, whereas in females deposition fractions of comparable aggregates amount to 64.1% and 40.4%. In the bronchial airways deposition probabilities and aggregate sizes are characterized by a positive correlation. Concretely speaking, small aggregates deposit by 20.4% (males) and 20.9% (females), whilst large aggregates accumulate by 44.6% (males) and 43.2% (females). A very similar tendency can be determined for the alveolar region, where deposition of small aggregates amounts to 1.68% (males) and 1.58% (females), whilst deposition of large aggregates adopts values of 14.9% (males) and 18.4% (females).

Regarding the deposition of variably shaped and sized nanoaggregates in single airway generations of the respiratory tract, model predictions are illustrated in *Figure 4*. Smallest particulate structures (10 steps) commonly deposit from generation 1 to 21, whereby in male lungs maximal deposition occurs in generations 10 and 11 and

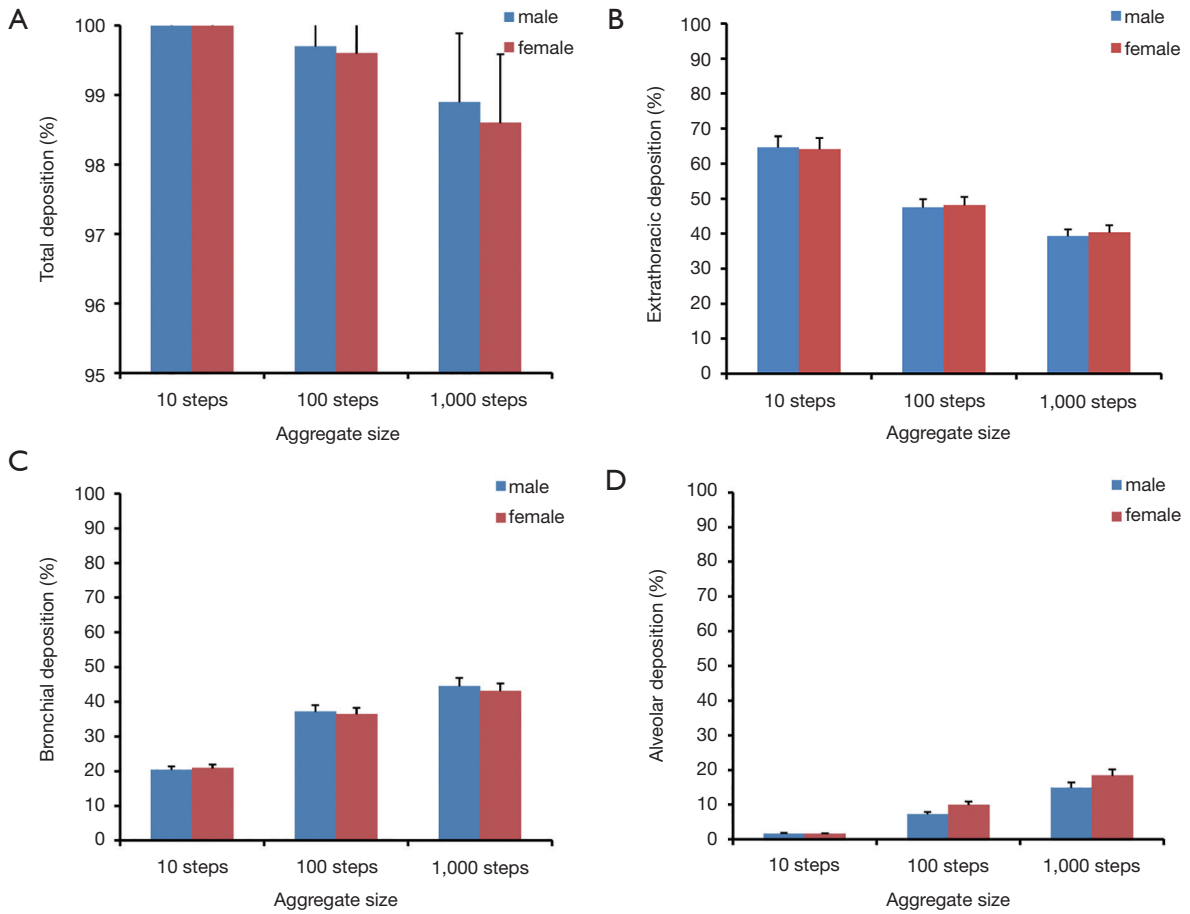

Figure 3 Total and regional deposition (mean ± standard deviation) of nanoaggregates with different complexity in the respiratory tract of males and females. (A) Total deposition; (B) extrathoracic deposition; (C) bronchial deposition; (D) alveolar deposition.

adopts values of 2.02%, respectively. In female lungs the deposition maximum is located in generation 11, thereby assuming a value of 2.08%. In the case of nanoaggregates produced by 100 random-walk steps deposition in single airway generations is characterized by a significant enhancement with respect to the smallest particles. Therefore, deposition ranges from 0.009% (generation 22) to 3.94% (generation 13) in male lungs, but from 0.03% (generation 22) to 4.01% (generation 15) in the respiratory tract of female subjects. Nanoaggregates modeled by 1,000 random-walk steps are marked by a further increase of their generation-by-generation deposition. Concretely speaking, deposition of these complex particulate structures varies between 0.065% (generation 23) and 5.09% (generation 15) in the case of male subjects, whereas in female subjects such aggregates deposit by 0.052% (generation 23) to 5.43% (generation 16).

Discussion and conclusions

As demonstrated by previous studies (3-7), the ambient atmosphere among other contains complex aggregates of the micro- and nano-scale, which are characterized by highly specific aerodynamic properties. The phenomenon of aggregation mainly concerns diesel soot and other particles emerging from incomplete combustion processes. In addition, also particles carrying an electric charge or being marked by increased hygroscopicity may be subjected to respective growth processes resulting in the formation of clusters or chains (1-8,17-19). Currently, a multitude of inhalable aggregates were categorized as serious health hazards (30-32). Therefore, advanced knowledge on the transport and deposition behavior of such particulate structures in the human respiratory tract has to be evaluated as essential for effective assessment of health risks. The present contribution could clearly demonstrate

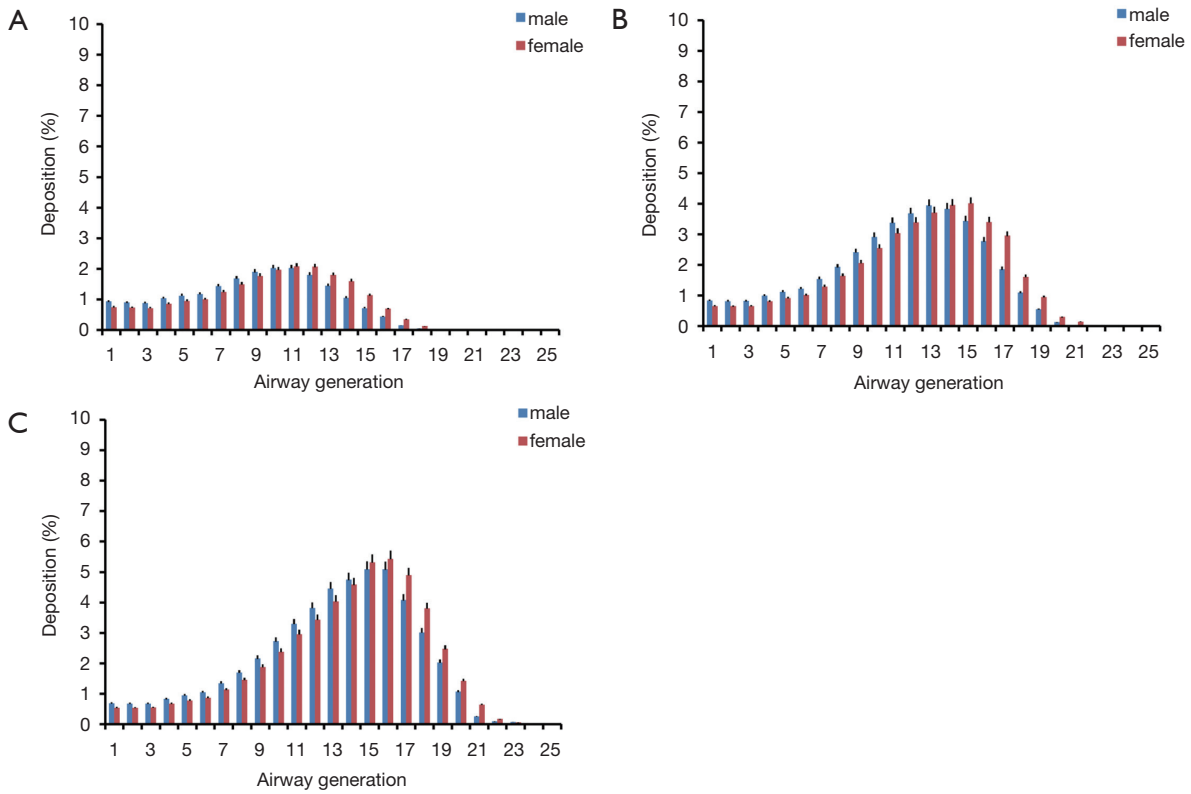

Figure 4 Generation-by-generation deposition of different nanoaggregates in male and female lungs. (A) Ten random-walk steps; (B) 100 random-walk steps; (C) 1,000 random-walk steps.

that aggregates belonging to the nano-scale possess the ability the reach more peripheral lung regions (small ciliated airways, alveoli) in rather high amounts. These compartments of the respiratory system, however, are distinguished by increased susceptibility for particle-tissue interactions with respect to the bronchial airways of the upper lung, where fast innate defense mechanisms act upon the particles (33-47).

As could be clearly demonstrated by the theoretical results of this contribution, deposition of nanoaggregates is subject to a continuous displacement from upper to lower lung regions with increasing size of the particulate structures (*Figures 3*,*4*). Brownian motion represents the main deposition force exerting on the particles, but exhibits a negative correlation with particle size (3-10,19,29). Since larger aggregates are marked by significantly lower deposition forces, they are able to cover longer distances within the respiratory tract, before they collide with the bronchial or alveolar wall (20,29). An enhancement of the inhalation flow rate, as it occurs by switching from sitting to light-work breathing, results in a further increase of the axial particle transport distance, so that the fraction of exhaled aggregates becomes remarkably enhanced (21-26). It has to be noted in this context that deposition behavior of highly anisometric particles such as aggregates, platelets or fibers considerably differs from that of volume-equivalent spheres (1-15). In the present study volume-equivalent diameters of the theoretically modeled aggregates exceed the related aerodynamic diameters by 10% to 30%. This means that volume-equivalent spheres exhibit higher peripheral deposition fractions than aggregates. On the other hand, they are characterized by decreased total deposition fractions (20,29).

Comparison of nanoaggregate behavior in the male lung with that in the female one came to expected results. Whilst total, extrathoracic and bronchial deposition of variably sized aggregates is slightly lower in women than in men, alveolar deposition is significantly increased in female lungs with respect to male lungs (*Figure 3*). This phenomenon is also reflected in the generation-by-generation deposition graphs, where deposition maxima in female lungs occur in more distal airway generations than those in male lungs.

The results can be mainly led back to gender-specific differences of airway morphometry and breathing behaviour which themselves influence the effectivity of Brownian motion (29).

Nanoaggregates deposited on the epithelial walls of airways and alveoli undergo various size-dependent clearance mechanisms. In the bronchial structures mucociliary transport as well as transepithelial clearance may be evaluated as most essential (33-47). Thereby, removal of particulate substances towards the lymphatic/vascular system may be finished within several minutes to hours (42). In the alveolar region transcytosis represents the main clearance mechanism, since macrophages are not able to detect and phagocytize particles of the nanoscale. If the aggregates are stored in epithelial cells and bound to intracellular structures, they may induce intracellular signal cascades resulting in malignant cellular transformations (24,42).

The results of the present study recommend further theoretical examinations of nanoaggregates, since these particles seem to play an important role in pulmonology.

Acknowledgments

Funding: None.

Footnote

Conflicts of Interest: The author has completed the ICMJE uniform disclosure form (available at http://dx.doi.org/10.21037/jphe.2018.04.02). The author has no conflicts of interest to declare.

Ethical Statement: The author is accountable for all aspects of the work in ensuring that questions related to the accuracy or integrity of any part of the work are appropriately investigated and resolved.

References

1. Fuchs NA. The Mechanics of Aerosols. New York: Pergamon Press, 1964.
2. Kasper G. Dynamics and measurement of smokes. I Size characterization of nonspherical particles. Aerosol Sci Technol 1982;1:187-99.
3. DeCarlo PF, Slowik JG, Worsnop DR, et al. Particle morphology and density characterization by combined mobility and aerodynamic diameter measurements. Aerosol Sci Technol 2004;38:1185-205.
4. Sturm R. Theoretical models for dynamic shape factors and lung deposition of small particle aggregates originating from combustion processes. Z Med Phys 2010;20:226-34.
5. Sturm R. Theoretical deposition of carcinogenic particle aggregates in the upper respiratory tract. Ann Transl Med 2013;1:25.
6. Sturm R. Spatial visualization of theoretical nanoparticle deposition in the human respiratory tract. Ann Transl Med 2015;3:326.
7. Sturm R. Deposition of ultrafine particles with various shapes in the human alveoli—a model approach. Comp Math Biol 2016;5:4.
8. Sturm R, Hofmann W. A computer program for the simulation of fiber deposition in the human respiratory tract. Comput Biol Med 2006;36:1252-67.
9. Högberg SM. Modeling nanofiber transport and deposition in human airways. Lulea University of Technology, 2010.
10. Sturm R. A theoretical approach to the deposition of cancer-inducing asbestos fibers in the human respiratory tract. TOLCJ 2009;2:1-11.
11. Sturm R. Nanotubes in the human respiratory tract - Deposition modeling. Z Med Phys 2015;25:135-45.
12. Sturm R. A stochastic model of carbon nanotube deposition in the airways and alveoli of the human respiratory tract. Inhal Toxicol 2016;28:49-60.
13. Sturm R, Hofmann W. Theoretical calculations of the deposition of non-spherical particles in the upper airways of the human lung. Z Med Phys 2009;19:38-46.
14. Sturm R, Hofmann W. A theoretical approach to the deposition and clearance of fibers with variable size in the human respiratory tract. J Hazard Mat 2009;170:210-8.
15. Sturm R. A computer model for the simulation of fiber-cell interaction in the alveolar region of the respiratory tract. Comput Biol Med 2011;41:565-73.
16. Sturm R. Inhaled nanoparticles. Phys Today 2016;69:70-1.
17. Willeke K, Baron PA. Aerosol measurement. New York:

John Wiley, 1993.
18. Hinds WC. Aerosol Technology: Properties, Behavior, and Measurement of Airborne Particles. New York: John Wiley, 1999.
19. Sturm R. Computer-aided generation and lung deposition modeling of nano-scale particle aggregates. Inhal Toxicol 2017;29:160-8.
20. Koblinger L, Hofmann, W. Monte Carlo modeling of aerosol deposition in human lungs. Part I: Simulation of particle transport in a stochastic lung structure. J Aerosol Sci 1990;21:661-74.
21. Hofmann W, Sturm R, Winkler-Heil R, et al. Stochastic model of ultrafine particle deposition and clearance in the human respiratory tract. Radiat Prot Dosimetry 2003;105:77-80.
22. Hofmann W, Bolt L, Sturm R, et al. Simulation of three-dimensional particle deposition patterns in human lungs and comparison with experimental SPECT data. Aerosol Sci Technol 2005;39:771-81.
23. Sturm R, Hofmann W. Stochastic model for the spatial visualization of particle-deposition patterns in the lung and their significance in lung medicine. Z Med Phys 2006;16:140-7.
24. Sturm R. Theoretical and experimental approaches to the deposition and clearance of ultrafine carcinogens in the human respiratory tract. Thorac Cancer 2011;2:61-8.
25. Sturm R. A computer model for the simulation of nonspherical particle dynamics in the human respiratory tract. Phys Res Int 2012;2012:1-11.
26. Sturm R. Theoretical deposition of nanotubes in the respiratory tract of children and adults. Ann Transl Med 2014;2:6.
27. Sturm R, Hofmann W. 3D-Visualization of particle deposition patterns in the human lung generated by Monte Carlo modeling: methodology and applications. Comput Biol Med 2005;35:41-56.
28. Sturm R. Modeling the deposition of bioaerosols with variable size and shape in the human respiratory tract–A review. J Adv Res 2012;3:295-304.
29. International Commission on Radiological Protection (ICRP). Human respiratory tract model for radiological protection, Publication 66. Oxford: Pergamon Press, 1994.
30. Peters A, Wichmann HE, Tuch T, et al. Respiratory effects are associated with the number of ultrafine particles. Am J Respir Crit Care Med 1997;155:1376-83.
31. Seaton A, MacNee W, Donaldson K, et al. Particulate air pollution and acute health effects. Lancet 1995;345:176-8.
32. Rojas M, Marie B, Vignaud JM, et al. High DNA damage by benzo[a]pyrene 7,8-diol-9,10-epoxide in bronchial epithelial cells from patients with lung cancer: comparison with lung parenchyma. Cancer Lett 2004;207:157-63.
33. Möller W, Felten K, Sommerer K, et al. Deposition, retention, and translocation of ultrafine particles from the central airways and lung periphery. Am J Respir Crit Care Med 2008;177:426-32.
34. Sturm R, Hofmann W. Mechanistic interpretation of the slow bronchial clearance phase. Radiat Prot Dosimetry 2003;105:101-4.
35. Hofmann W, Sturm R. Stochastic model of particle clearance in human bronchial airways. J Aerosol Med 2004;17:73-89.
36. Sturm R, Hofmann W. A multi-compartment model for slow bronchial clearance of insoluble particles--extension of the ICRP human respiratory tract models. Radiat Prot Dosimetry 2006;118:384-94.
37. Sturm R. A computer model for the clearance of insoluble particles from the tracheobronchial tree of the human lung. Comput Biol Med 2007;37:680-90.
38. Sturm R. A three-dimensional model of tracheobronchial particle distribution during mucociliary clearance in the human respiratory tract. Z Med Phys 2013;23:111-9.
39. Sturm R, Hofmann W, Scheuch G, et al. Particle clearance in human bronchial airways: comparison of stochastic model predictions with experimental data. Ann Occup Hyg 2002;46:329-39.
40. Sturm R, Hofmann W. Stochastic modeling predictions for the clearance of insoluble particles from the tracheobronchial tree of the human lung. Bull Math Biol 2007;69:395-415.
41. Sturm R. Age-dependence and intersubject variability of tracheobronchial particle clearance. Pneumon 2011;24:77-84.
42. Geiser M, Rothen-Rutishauser B, Kapp N, et al. Ultrafine particles cross cellular membranes by nonphagocytic mechanisms in lungs and in cultured cells. Environ Health Perspect 2005;113:1555-60.
43. Sturm R. Theoretical models of carcinogenic particle deposition and clearance in children's lungs. J Thorac Dis 2012;4:368-76.
44. Sturm R. Clearance of carbon nanotubes in the human respiratory tract-a theoretical approach. Ann Transl Med 2014;2:46.
45. Sturm R. An advanced mathematical model of slow bronchial clearance in the human respiratory tract. Comp

Math Biol 2016;5:2.
46. Sturm R. Carbon Nanotubes in the Human Respiratory Tract-Clearance Modeling. Ann Work Expo Health 2017;61:226-36.
47. Sturm R. Inhalation of nanoplatelets - Theoretical deposition simulations. Z Med Phys 2017;27:274-84.

doi: 10.21037/jphe.2018.04.02
Cite this article as: Sturm R. Theoretical deposition of random walk-generated nanoaggregates in the lungs of healthy males and females. J Public Health Emerg 2018;2:16.

